Kinetics and Mechanism of Oxygen-Independent Hydrocarbon Hydroxylation by Ethylbenzene Dehydrogenase†

Maciej Szaleniec,‡ Corina Hagel,§ Maurycy Menke,‡ Pawel Nowak,‡ Malgorzata Witko,‡ and Johann Heider*,§

Institute of Catalysis and Surface Chemistry, Polish Academy of Sciences, Niezapominajek 8, 30-239 Krakow, Poland, and Fachbereich Biologie, Institut für Mikrobiologie und Genetik, Technische Universität Darmstadt, Schnittspahnstrasse 10, D-64287 Darmstadt, Germany

Received April 17, 2007

ABSTRACT: Ethylbenzene dehydrogenase (EBDH) from the denitrifying bacterium *Azoarcus* sp. strain EbN1 (to be renamed *Aromatoleum aromaticum*) catalyzes the oxygen-independent, stereospecific hydroxylation of ethylbenzene to (*S*)-1-phenylethanol, the first known example of direct anaerobic oxidation of a nonactivated hydrocarbon. The enzyme is a trimeric molybdenum/iron−sulfur/heme protein of 155 kDa that is quickly inactivated in air in its reduced state. Enzyme activity can be coupled to ferricenium tetrafluoroborate, providing a convenient way for kinetic measurements. EBDH exhibits activity with a wide range of ethylbenzene analogues, which were analyzed for their kinetic parameters, stoichiometry, and formed products. The reactivity was correlated to the chemical structures by a quantitative structure−activity relationship (QSAR) model. On the basis of these results, quantum chemical calculations of ΔG^{298} for formation of carbocations of the respective substrates were performed and used in reactivity analysis. A putative reaction mechanism is proposed on the basis of the experimental results and theoretical considerations. Finally, the enzyme reaction has been established in an electrochemical reactor, allowing sustained enzymatic reaction and potential technical applications of the enzyme.

Mononuclear molybdenum enzymes constitute a fairly large class of biocatalysts that contain the molybdenum cofactor in their active centers, which consists of one Mo atom ligated to one or two molybdopterins. These enzymes are classified into three major families on the basis of structural differences and the mode of binding of the Mo cofactor, namely, the xanthine oxidase family, the sulfite oxidase family, and the DMSO reductase family (*1*).

The recently discovered molybdoenzyme ethylbenzene dehydrogenase (EBDH)[1] belongs to the DMSO reductase family (*2*−*4*) and exhibits the highest sequence similarities to selenate reductase of *Thauera selenatis* (*5*), dimethyl sulfide dehydrogenase of *Rhodovulum sulfidophilum* (*6*), perchlorate and chlorate reductases of *Dechloromonas* sp., and nitrate reductases from archaebacteria and eubacteria (*7*, *8*). It catalyzes the oxygen-independent oxidation of ethylbenzene to (*S*)-1-phenylethanol as the initial step of anaerobic ethylbenzene degradation by the denitrifying bacterial strains EbN1, EB-1, and PbN1 (*2*, *3*). EBDH consists of three subunits of 96, 43, and 23 kDa and contains a molybdenum cofactor and a heme *b*559 cofactor linked by a linear row of five iron−sulfur clusters (*9*). EBDH is synthesized exclusively in cells grown anaerobically on ethylbenzene and has been identified as a soluble periplasmic protein that is transported over the cytoplasmic membrane via the twin-arginine transport system (*3*, *4*). Remarkably, the purified enzyme is quickly inactivated by atmospheric oxygen, although it is not affected by air in crude extracts (*3*). Elucidation of the detailed role of EBDH in biomineralization of ethylbenzene, a major component of crude oil, will help to understand the recovery of polluted ecosystems. EBDH also promises potential applications in the chemical and pharmaceutical industry, as the enzyme is enantioselective and seems to react with a relatively wide spectrum of substrates (*2*, *3*). In our study we have further explored the reactivity of EBDH with different compounds and have identified 20 substrates and 9 inhibitors. We identified the products formed from alternative substrates by chromatographic analysis and MS experiments and performed detailed kinetic studies that allow to propose a potential mechanism of ethylbenzene oxidation.

EXPERIMENTAL PROCEDURES

Enzyme Purification. Ethylbenzene dehydrogenase was purified from ethylbenzene grown cells of strain EbN1 ("*Aromatoleum aromaticum*"), which was isolated by Rabus and Widdel (*4*). Growth of the organism, extract preparation, and EBDH purification were performed as described previ-

† This research has been supported by the Polish Ministry of Science and Higher Education under Grant KBN/SGI2800/PAN/037/2003 and Scientific Network EKO-KAT and by the Deutsche Forschungsgemeinschaft (He2190/4-1). M.S. acknowledges a Ph.D. grant of the Polish Academy of Sciences.

* To whom correspondence should be addressed: phone, +49-6151-16-5203; fax, +49-6151-16-2956; e-mail, heider@bio.tu-darmstadt.de.

‡ Polish Academy of Sciences.

§ Technische Universität Darmstadt.

[1] Abbreviations: DFT, density functional theory; EBDH, ethylbenzene dehydrogenase; HOMO, highest occupied molecular orbital; LC-MS, liquid chromatography−mass spectroscopy; LUMO, lowest unoccupied molecular orbital; MLR, multiple linear regression; PRESS, the sum over square deviations for all compounds between actual and predicted values of the independent variable $\sum(y_i - y)^2$; QSAR, quantitative structure−activity relationship; SCE, standard calomel electrode.

10.1021/bi700633c CCC: $37.00
Published on Web 06/02/2007

ously (*3*, *10*). The deactivation of the enzyme during aerobic purification was prevented by the addition of ferricenium tetrafluoroborate to the buffers to keep the protein oxidized (*10*). Enzyme activity was determined spectrophotometrically in 100 mM Tris-HCl buffer (pH 7.5) containing 0.1 mM ferricenium tetrafluoroborate at 30 °C. Decrease of absorption of the ferricenium ion was followed at 290 nm. The difference of absorption coefficients at 290 nm between the oxidized and reduced forms was experimentally determined as $\Delta\epsilon = 6200\ M^{-1}\ cm^{-1}$.

Kinetic Measurements. The reaction system contained ethylbenzene or a related compound and ferricenium tetrafluoroborate as an electron acceptor. Kinetic parameters of ferricenium were obtained by nonlinear fitting of activity data to the Michaelis−Menten equation from experiments with a fixed concentration of ethylbenzene (60 μM); those for ethylbenzene and other substrate analogues were obtained from experiments with a fixed ferricenium concentration (100 μM). For each experiment, the enzyme was assayed in duplicate measurements at more than 10 concentrations of the variable substrate. The k_{cat} of ethylbenzene was always measured as a control along with those of alternative substrates. The same reaction stoichiometry (1 substrate per 2 ferricenium) was assumed in the case of all monoethyl-substituted substrates. As the apparent K_m of ethylbenzene was very low (less than 1 μM), stopped-flow spectrometry was used for determination of the kinetics of this substrate (Applied Photophysics).

Analytical Methods. (A) HPLC Sample Preparation. Solutions of standard compounds were prepared in aqueous acetonitrile (50%). Samples of reaction mixtures were prepared by addition of acetonitrile to 50% (v/v), which leads to precipitation of the enzyme and terminates the reaction. The coagulated enzyme was removed by centrifugation for 8 min at 14000 rpm. Aliquots of the supernatant (10 or 20 μL) were injected in duplicate for each analysis. Reactions to be analyzed by LC-MS were conducted in an almost UV-transparent ammonium bicarbonate buffer system (100 mM NH_4HCO_3, pH 7.8) instead of Tris-HCl. Alternatively, solid-phase extraction on SPE C18, CN, or Polar+ columns (Baker) was used to concentrate and desalt samples before analysis.

(B) HPLC Conditions. The analyses were performed on reversed-phase amide columns (Ascentis) using water/acetonitrile as the mobile phase at a flow rate of 0.43 mL/min with different gradient programs, depending on the substance. Elution of the column usually started at 20−40% of acetonitrile and extended to 70−75% of acetonitrile. Generally, the separation program started with 2 min of isocratic flow with low acetonitrile content (20−40%), followed by a rapid gradient up to 40−60% of acetonitrile, another isocratic section (over 6−10 min), and finally another gradient up to 75% of acetonitrile. Ferricenium tetrafluoroborate, buffer compounds, and polar products eluted during the first isocratic part of the gradient program and substrates during the second isocratic part, while ferrocene eluted in the last section. The aromatic compounds were detected by UV absorbance at the following wavelengths, depending on the respective reaction mixtures: (i) 210, 215, and 260 nm (reactions with ethylbenzene), (ii) 230 and 278 nm (reactions with alkylphenols), (iii) 235 nm (reactions with 2-ethylthiophene), (iv) 280.5 nm (reactions with 2-ethylfuran), and (v) 220 and 261 nm (reactions with 1,4-diethylbenzene). For quantitative analysis of ethylbenzene reaction mixtures, calibration curves were established with standard solutions of ethylbenzene and 1-phenylethanol.

(C) LC-MS Conditions. Analyses were conducted on an instrument (Agilent 1100 System LC/MSD Quad VL) equipped with a diode array detector and either atmospheric pressure chemical ionization (APCI) in the positive ion mode or atmospheric pressure electrospray ionization (ESI) in the negative mode. Developing of the columns was described above, except of the addition of 0.1% of formic acid to the mobile phase.

(D) GC-MS Conditions. GC-MS analyses were performed on a Varian 3400 GC instrument coupled with an Incos 500 mass spectrometer (ThermoFinnigan). Separation was conducted on a (5% phenyl)-methylpolysiloxane column (Agilent DB-5.625) with helium as carrier gas. The ionization was achieved by electron impact at 22 eV. The thermal program varied depending upon the substance analyzed. Generally, the temperature was raised from a starting point at 60−100 °C to an end point at 180 °C at 25−30 °C/min.

(E) Protein Concentration. Protein concentration was quantified by the Coomassie dye binding assay with BSA as standard.

(F) Electrochemical Methods. Electrochemically sustained oxidation of ethylbenzene was performed anaerobically at 45 °C in a glass tube reactor (10 mL), equipped with a magnetic stirrer, a platinum wire working electrode, saturated calomel reference electrode (SCE), and Ag/AgCl counter electrode. To avoid the interference of Cl^- ions, the counter electrode was separated from the reaction space by a glass wool stopcock. The working potential was set to 450 mV against the SCE ($E^{0\prime} = +694$ mV). The potential was controlled by a digital potentiostat (1286 Electrochem Interface, Solatron). The reaction was performed in 8 mL of 100 mM Tris-HCl, pH 7.5, containing 165 μM ferricenium and 78 μg of EBDH. The reaction was started by injection of 50 μL of a solution of ethylbenzene in *tert*-butyl alcohol (0.08 M, end concentration 500 μM). Under these conditions, the reaction was followed for 4.5 h. Samples of the reaction mixture (25 μL) were collected at chosen time points, and the enzymatic reaction was stopped by addition of 25 μL of acetonitrile. The concentration of 1-phenylethanol was measured by HPLC.

Quantum Chemical Calculations. All quantum chemical calculations were conduced at B3LYP/6-31G(d,p) level of theory in the Gaussian 03 suite of programs (*11*). The geometries of substrates and their carbocations were optimized in the gas phase at 0 K. In the case of carbocations of 2-ethyl compounds, both *E* and *Z* isomers were considered. As it is not apparent which conformation is present in the active center, an average value of energies for both conformers was used for analysis. The vibration analysis was performed in order to verify complete optimization and to obtain the zero point vibrational corrections necessary for thermochemical calculations (298 K, 1 atm). As a result, changes in Gibbs free energy ΔG^{298} of hydride subtraction and carbocation formation were calculated for all compounds. While these gas-phase ΔG^{298} values did not prove to be good models of enzyme-catalytic reactions, differences in ΔG^{298} between substrates ($\Delta\Delta G^{298}$), taking ΔG^{298} for ethylbenzene as a reference, supplied information on stabilization effects

introduced by modification of the aromatic system. Each compound was also characterized by the dipole moment, μ, and the frontier orbital energies, i.e., E_{LUMO} (as an approximation of electron affinity) and E_{HOMO} (as an approximate measure of ionization potential), and absolute hardness η, half of the energy difference between E_{LUMO} and E_{HOMO}. The energies of orbitals were provided in electron volts, and to avoid sign changes between occupied and unoccupied orbitals, their values were elevated by 6.42 eV (rendering E^{HOMO} of ethylbenzene equal to 0 eV).

Quantitative Structure−Activity Relationship. A commercially available multi linear regression package (Statistica 7.1, Statsoft) was used to construct several linear quantitative structure−activity relationship (QSAR) models describing reaction rates with 13 different substrate analogues. Relative kinetic rate constants (scaled in percent relative to the reaction rate with ethylbenzene) were converted into logarithmic scale and correlated with linear combinations of different molecular descriptors of substrate analogues. The best model developed by stepwise regression was obtained with a linear combination of the Taft steric constants E_s, hydrophobic constant π (*13*), dipole moment (μ), and HOMO and LUMO energies (E^{HOMO} and E^{LUMO}). Alternatively, instead of E^{HOMO}, the Hammett σ^+ constant was used, which describes electronic effects in systems with positively charged transition states where direct resonance between reaction centers and substituents takes place (*14*), or calculated gas-phase Gibbs free energies of carbocation formation reactions ($\Delta\Delta G^{298}$). The obtained models were tested by internal cross-validation performed in the Cerius^2 package (*15*).

RESULTS

Kinetics of Ethylbenzene Oxidation. Ethylbenzene is the native substrate of EBDH and as such exhibits a very low K_m value that was not measurable by conventional enzyme testing (*3*). Therefore, we analyzed the steady-state kinetics of EBDH by stopped-flow spectrophotometry using very low concentrations of ethylbenzene. The results were fitted by nonlinear regression to the Michaelis−Menten equation, yielding an apparent K_m value of ethylbenzene of 0.45 ± 0.19 μM (Figure S1 of the Supporting Information). To obtain the kinetic parameters of the electron acceptor, tests were performed with 60 μM ethylbenzene in the presence of different concentrations of ferricenium tetrafluoroborate (from 30 to 250 μM). These assays yielded an apparent K_m value of the ferricenium ion of 28.3 ± 3.9 μM (Figure S2 of the Supporting Information).

EBDH Substrate Spectrum. Previous results on the substrate spectrum of EBDH (*2*, *3*) suggested that the enzyme is capable of oxidizing several compounds containing ethyl or propyl groups attached to aromatic (or unsaturated aliphatic) systems. Substituents of alternative substrates may stabilize transition states and affect reaction kinetics. Therefore, in order to elucidate possible reaction mechanisms of EBDH, we investigated the reactivity of a wide scope of aromatic and heteroaromatic substrate analogues (Figure S3 of the Supporting Information). The studied compounds consisted of three groups, namely, nonactivated hydrocarbons (2-, 3-, and 4-ethyltoluene, 1,4-diethylbenzene, *n*-propyl- and isopropylbenzene, 2-ethylnaphthalene, and 4-ethylbiphenyl), hydrocarbons with non-carbon substituents of the aromatic ring (2-, 3-, and 4-ethylphenol, 4-propylphenol, 2- and 4-ethylaniline, 4-ethylanisole, and 4-fluoroethylbenzene), and heteroaromatic compounds (2-, 3-, and 4-ethylpyridine, 2-ethylpyrazine, 2-ethylpyrrole, 2-ethylfuran, and 2-ethylthiophene). Of the hydrocarbon substrates, all ethyltoluene isomers, 1,4-diethylbenzene, *n*-propylbenzene, 4-ethylbiphenyl, and 2-ethylnaphthalene were oxidized by EBDH at different rates (see Table 1), whereas isopropylbenzene was not. A two-electron oxidation was confirmed for several of the monoethyl-substituted compounds by assessing the stoichiometry with ferricenium, whereas 1,4-diethylbenzene seemed to be oxidized at both ethyl groups, revealing a four-electron stoichiometry (Table 1). All investigated substituted substrates with heteroatom substituents were oxidized by EBDH. The reactivity of the various ethylphenol isomers was markedly different: 4-ethylphenol was oxidized 2.5-fold faster than the native substrate ethylbenzene, whereas 2- and 3-ethylphenol were oxidized successively slower. Also, 4-propylphenol was oxidized at a 1.8-fold faster rate than ethylbenzene and 12-fold faster than *n*-propylbenzene. The apparent K_m values of ethylphenols were diverse, but significantly higher than that of ethylbenzene, ranging from 40.5 μM in the case of 4-ethylphenol to 9.3 μM for 3-ethylphenol and 5.2 μM for 2-ethylphenol, respectively.

Table 1: Summary of Kinetic Measurement Results[a]

substrate	k_{cat} (%)	app K_m (μM)	k_{cat}/K_m ($s^{-1}M^{-1}$)	stoichiometry ferricenium to substrate ratio	product identified
ethylbenzene	100	0.45	586365	2.2	+
1,4-diethylbenzene	35	nm[b]		4.9	+
n-propylbenzene	14	nm			+
isopropylbenzene	0	nb[c]			
2-ethyltoluene	3.8	nm			nm
3-ethyltoluene	10	nm			nm
4-ethyltoluene	28	nm			+
2-ethylnaphthalene	9.3	nm			nm
4-ethylbiphenyl	30	nm			+
4-fluoroethylbenzene	15	nm			nm
2-ethylphenol	55	5.18	32364	2.5	+
3-ethylphenol	19	9.27	24615	2.3	+
4-ethylphenol	251	40.47	16533	2.3	+
4-propylphenol	175	nm			+
4-ethylanisole	22	nm			+
2-ethylaniline	92	24.30	10049		nm
4-ethylaniline	130	nm			nm
2-ethylpyrazine		nb			
3-ethylpyridine	16	1.86	23528		nm
2-ethylfuran	130	24.69	14026		+
2-ethylthiophene	236	66.46	9442		+
2-ethylpyrrole	228	2.32	261262		nm

[a] Kinetic rate constants are provided in relative scale. Control assays with ethylbenzene were performed in parallel to all kinetic experiments and set as 100%. These activities ranged between 80 and 160 nmol mg^{-1} min^{-1}, depending on the batch of enzyme. Apparent K_m values were obtained with 100 μM ferricenium tetrafluoroborate at 30 °C. The stoichiometry was calculated from activity assays with a limited amount of substrate (from 2 to 60 μM) that were run to the completion of the reaction; it is given as ratio of conversion of ferricenium to substrate added. Identified products by GC-MS or LC-MS are indicated. The error range for kinetic rate constants did not exceed 10% of the value, while in the case of apparent K_m values, errors usually were in the range of 10−30%. Higher errors (40−200%) were observed for apparent K_m values below 5 μM. Errors in the stoichiometry factors were in the range of 1−9%. [b] nm, not measured. [c] nb, no binding.

Table 2: Summary of GC-MS and LC-MS Analysis of Reaction Products[a]

substrate	substrate mol mass	product	GC-MS M^+	LC-MS APCI M^+	LC-MS ESI $[M - H]^-$
ethylbenzene	106	1-phenylethanol	122 (+O)	122 (+O)	
propylbenzene	120	1-phenylpropanol	136 (+O)		
4-ethyltoluene	120	1-(4-methylphenyl)ethanol	136 (+O)		
1,4-diethylbenzene	134	1-(4-ethylphenyl)ethanol	150 (+O)	150 (+O)	
		1,1′-(1,4-phenylene)diethanol		166 (+2O)	
1,4-ethylbiphenyl	182	1-(1,1′-biphenyl-4-yl)ethanol	198 (+O)		
4-ethylanisole	136	1-(4-methoxyphenyl)ethanol	152 (+O)		
2-ethylthiophene	112	1-thien-2-ylethanol	128 (+O)	128 traces (+O)	
2-ethylfuran	96	1-(2-furyl)ethanol		112 (+O)	
2-ethylphenol	122	2-(1-hydroxyethyl)phenol			137 (+O)
3-ethylphenol	122	3-(1-hydroxyethyl)phenol	138 (+O)		137 (+O)
4-ethylphenol	122	4-(1-hydroxyethyl)phenol			137 (+O)
4-propylphenol	136	4-(1-hydroxypropyl)phenol			151 (+O)
ethylidenecyclohexane	110	multiple products not identified	124 (+O − 2H)		
			126 (+O)		
			128 ($+H_2O$)		

[a] The substrate section of the table provides substrate names with their molecular masses. The product section gives names of the respective products along with experimentally obtained molecular ion masses (M^+) as obtained from GC-MS electron impact, positive APCI LC-MS ionization, and quasi-molecular ion masses $[M - H]^-$ from negative ESI LC-MS ionization. Note that the M^+ values correspond to the respective molecular masses of products; those of $[M - H]^-$ are *m*/*z* 1 smaller. All recorded mass differences between substrates and products correspond to one added oxygen (*m*/*z* 16), as indicated by (+O).

The studied isomers of ethylaniline behaved similarly, with 4-ethylaniline oxidized 1.4-fold faster than ethylbenzene and 2-ethylaniline slightly slower. For the latter, an apparent K_m value was established at 24.3 μM. The methoxy derivative of ethylbenzene, 4-ethylanisole, was only oxidized with a rate comparable to 4-ethyltoluene. Lastly, 4-fluoroethylbenzene was oxidized only at 15% of relative rate of ethylbenzene. In the last group of heterocyclic compounds, three excellent substrates have been found which were oxidized faster than ethylbenzene, namely, 2-ethylpyrrole, 2-ethylfuran, and 2-ethylthiophene (Table 1). 3-Ethylpyridine exhibited moderate activity (Table 1), whereas the other ethylpyridine isomers inhibited the reaction. 2-Ethylpyrazine was neither oxidized nor inhibitory for the enzyme. The lowest K_m values of these ethylbenzene analogues were recorded for 3-ethylpyridine (1.9 μM) and 2-ethylpyrrole (2.3 μM). In the case of 2-ethylfuran and 2-ethylthiophene K_m values equaled 24.7 and 66.5 μM, respectively. The only tested substrate with a saturated aliphatic ring was ethylidenecyclohexane, which exhibited only trace activity in the ferricenium-coupled assay (see below for product analysis). None of the K_m values of any substrate analogue came close to the extremely low level recorded for ethylbenzene.

Product Identification. In order to investigate whether ethylbenzene dehydrogenase converts all known substrates into secondary alcohols, the formation of reaction products has been examined by means of reversed-phase LC-MS and GC-MS. Only one major product peak was observed with any of the tested aromatic substrates. All of the products eluted at earlier HPLC retention times than the respective substrates, indicating increased polarity. Mass spectra of the various products were collected and verified their expected identity.

The reaction product of control reactions with ethylbenzene was identified as 1-phenylethanol on the basis of (i) retention time of the standard compound in GC-MS and HPLC, (ii) molecular ion mass of the product (LC-MS), and (iii) MS fragmentation pattern and its comparison with the mass spectra database (*16*). The conversion products of propylbenzene, 4-ethylanisole, and 4-ethyltoluene were identified by GC-MS based on deposited spectra of respective alcohol derivatives (Table 2). The other observed products of conversion reactions were identified on the basis of their molecular ion masses (in LC-MS analysis) and/or manual assessment of the fragmentation patterns (in GC-MS and APCI analysis), which had all of the characteristics expected for secondary alcohols (*17*) (Table 2). The analysis of the 1,4-diethylbenzene reaction mixture revealed 1-(4-ethylphenyl)ethanol (monohydroxylated) as a main product along with 1,1′-(1,4-phenylene)diethanol (doubly hydroxylated). The latter product is present in higher quantities when an excess of ferricenium over 1,4-diethylbenzene is provided (more than 2:1 molar ratios).

GC-MS of the reaction products of the alkylphenol isomers only allowed to identify 3-(1-hydroxyethyl)phenol as the product of 3-ethylphenol oxidation. However, consistent identification of all products formed from these substrates was possible by LC-MS analysis coupled with a negative ion mode of electrospray ionization (Table 2).

GC-MS analysis of a reaction mixture with ethylidenecyclohexane revealed trace amounts of five different product peaks with molecular ion masses of *m*/*z* 126, 128, and 124. The analysis of fragmentation patterns suggests hydroxylated unsaturated derivatives in the case of three products (M^+ *m*/*z* 126) and a hydratized saturated derivative in the case of one product (M^+ *m*/*z* 128). The fifth product (M^+ *m*/*z* 124) had some features of an unsaturated ketone, although that could not be confirmed without further investigations. Therefore, ethylidenecyclohexane apparently binds and reacts at the active site of the enzyme but is converted to an undefined mixture of compounds. Moreover, different types of reactions seem to take place, ranging from water addition to hydroxylations at different sites and possibly further oxidation of a hydroxylated intermediate.

Inhibition Studies. Several compounds were found to exert inhibitory effects on the enzyme. The identified inhibitors can be grouped into (i) products and product analogues such as (*S*)- and (*R*)-1-phenylethanol or 1-(2-naphthyl)ethanol, (ii) methyl-group-containing substrate analogues, such as toluene, 2-methylfuran, or 2-methylthiophene, (iii) some ethyl-

substituted aromatic compounds such as 1,2-diethylbenzene and 2- and 4-ethylpyridine, (iii) structural ethylbenzene analogues such as 4-ethylanisole, and finally (iv) small molecules such as H_2O_2.

Initial investigation on the inhibitory effects caused by the different compounds revealed that product analogues seem to be very weak inhibitors of ethylbenzene dehydrogenase. Half-maximum activity was recorded in the presence of 10 mM (*S*)-1-phenylethanol and 3 mM racemic 1-(2-naphthyl)-ethanol, respectively. Inhibition seems to be unaffected by the stereochemistry of the alcohol, judging by a very similar inhibitory effect caused by (*S*)- and (*R*)-1-phenylethanol. The tested inhibitors containing methyl groups exhibited medium inhibitory effects, decreasing the activity to 50% in a concentration range of 0.5−1 mM. Inhibitors containing ethyl groups showed diverse effects. 4-Ethylpyridine caused half-maximum inhibition at a concentration of 2 mM, whereas 2-ethylpyridine and 1,2-diethylbenzene had the same effect at concentrations of 100−200 μM. The inhibitory effect of anisole was similar to that of the latter compounds with half-maximum inhibition at a concentration of 100 μM. More detailed inhibition kinetics have been assessed for the product inhibition by (*S*)-1-phenylethanol. To this end, the ethylbenzene dehydrogenase was measured in the presence of different concentrations of inhibitor (1.3, 6.5, and 13 mM), and the data were fitted against the equations describing different modes of enzyme inhibition [performed by the Leonora software package (*18*)]. This revealed a competitive inhibition mechanism (Figure S4 of the Supporting Information) of (*S*)-1-phenylethanol with an inhibition constant K_i of 20 μM. The value of K_m derived from this curve fitting equaled 0.6 μM, confirming the value obtained in the direct determination.

EBDH is inactivated by exposure to air only in the reduced state, possibly due to generation of reactive oxygen species at the reduced heme cofactor (*3*). In contrast, it is oxygen-insensitive in the oxidized state. Therefore, we used the oxidized form of EBDH to determine whether it is indeed inactivated by active oxygen species like H_2O_2. Residual activities were measured after 5 min preincubation of the concentrated ethylbenzene dehydrogenase (12.5 μM) with different concentrations of H_2O_2, yielding 50% inactivation at 15 mM H_2O_2. The inactivation seems to be irreversible, as enzyme activity could not be restored after anaerobic reduction by 10 mM sodium dithionite.

Electrochemical Reactor. Possible applications of EBDH for synthesis of large concentrations of chiral alcohols are severely limited by the high price and low solubility of the electron acceptor ferricenium that is consumed in the reaction. Therefore, we tested whether the enzyme functions in an electrochemical cell that continuously regenerates the electron acceptor at the platinum mesh electrode. Ferricenium is reduced to ferrocene during the reaction and then reoxidized by the electrode, keeping its concentration constant. Moreover, the reaction can then conveniently be followed by recording the current of the electrochemical cell.

The experiment was performed under argon atmosphere in an electrochemical batch reactor using a 3-fold molar excess of ethylbenzene over ferricenium. The characteristic changes of the current during the experiment are shown in Figure 1. The reaction rate speeded up after injection of substrate and reached its maximum value after 40 min.

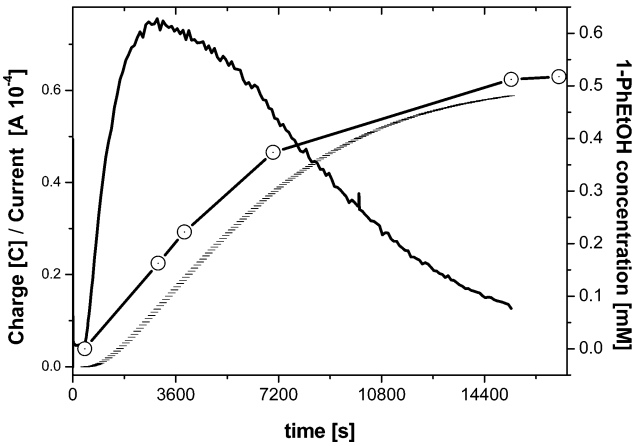

FIGURE 1: Changes of current (solid line), accumulation of charge transferred by the electrode in the reaction of ferrocene reoxidation and product (dashed line), and 1-phenylethanol concentration (circles) during the electrochemical experiment. The last measured value of 1-phenylethanol concentration was obtained after the electrochemical system was shut down and the reaction proceeded overnight with the remaining ferricenium.

Integration of the current curve over time yields a representation of the accumulation of charge that is proportional to ethylbenzene conversion to (*S*)-1-phenylethanol. Indeed, product formation over time, as determined by HPLC, followed the same kinetics (Figure 1).

The accumulation of charge and product showed an approximately linear rate during the first 2 h of the reaction. After that point, the reaction rate decreased, most probably due to inactivation and/or substrate depletion. Using this electrochemical system, we were able to convert 95% of the ethylbenzene present to 1-phenylethanol, as established by accumulated charge transferred and HPLC quantification.

QSAR Analysis. In order to quantify the variation in reactivity of different substrates, we performed quantitative structure−activity relationship (QSAR) analysis, assessing the determined reactivity with several molecular parameters of respective substrates. Because no satisfactory correlation was reached with any singular molecular parameter, multivariate regression was performed with combinations of molecular parameters for 13 compounds that shared the structural core of ethylbenzene.

The best fitting equation was obtained by combining the Taft steric constants E_s, the hydrophobic constants π, and three density functional theory (DFT) based descriptors: dipole moment (μ) and HOMO and LUMO energies (Figure 2). The R^2 value achieved with those descriptors was very high (0.96), which means that 96% of variance is explained by the model. The equation was cross-validated by leaving out single data sets ("leave-one-out cross-validation"), yielding an R^2 value of 0.9540 (PRESS = 0.14130).

$$\log k_{cat} = 1.37(\pm 0.23)E_s - 1.14(\pm 0.22)\pi - 1.69(\pm 0.19)\mu + 1.28(\pm 0.17)\mathrm{HOMO} - 1.7(\pm 0.18)\mathrm{LUMO} + 26.4 \quad (1)$$

$$R^2 = 0.9598;\ R = 0.9797;\ p = 5 \times 10^{-8}$$

The obtained equation shows that steric effects (E_s) decrease the reaction rate (E_s being more negative for larger substituents). The hydrophobicity parameter π and the dipole moment define an optimal range of polarization and hydro-

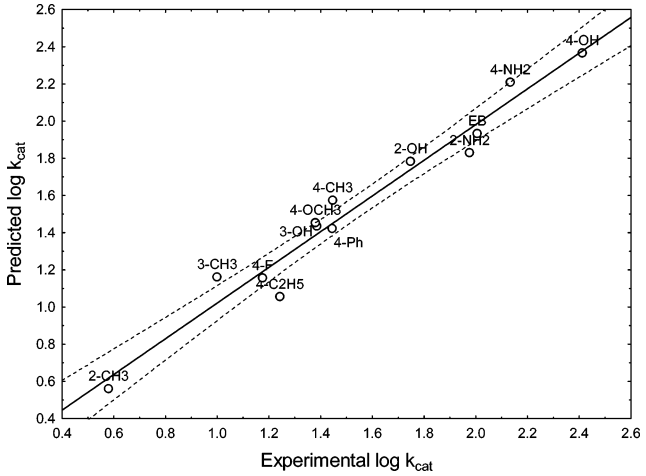

FIGURE 2: Correlation of predicted relative k_{cat} with experimental values in the MLR model (eq 1) ($R^2 = 0.9598$, $R = 0.9797$, $p = 5 \times 10^{-8}$, c-v $R^2 = 0.9540$, PRESS = 0.1413). Key: solid line, regression curve; dotted line, 95% confidence level. Labels describe localization of the substituent in respect to the ethylbenzene core (e.g., 4-Ph states for 4-ethylbiphenyl).

phobicity of the substrates. More hydrophobic substrates tend to have lower reaction rates, but also, on the other hand, smaller dipole moments yield faster reaction rates. The energies of frontier orbitals describe electronic features of the analyzed substrates. The DFT-derived LUMO and HOMO energies have a conceptual transfer into chemical concepts, such as ionization potential ($-E^{HOMO}$) and electron affinity ($-E^{LUMO}$), and, as a result, to absolute hardness (η = half of the energy difference between LUMO and HOMO) and softness ($S = 1/\eta$) (*19*, *20*).

The higher E^{HOMO} of a molecule, the less energy is required for its ionization, and the lower E^{LUMO} of a compound, the higher is its affinity for acquiring a new electron. Therefore, the effects of E^{HOMO} and E^{LUMO} in the equation can be interpreted as follows: the positive correlation of reaction rates with E^{HOMO} and their negative correlation with E^{LUMO} indicate that the reaction proceeds faster the easier the molecule is to ionize and the higher the electron affinity of the substrate is. The effects of E^{HOMO} and E^{LUMO} on the reaction kinetics seem to be contradictory at first sight but can be fully understood by the concept of chemical hardness η. Regrouping of eq 1 (eq S1 of the Supporting Information) indicates a correlation of increasing absolute hardness with lower reactivity, which can be explained by the higher ionization potential (and higher stability) and lower polarizability of the compounds, which are "hard" substrates (such as ethylbenzene) compared to "soft" substrates (such as 4-ethylphenol).

The HOMO energies correlate strongly with the Hammett constants σ^+ ($R = -0.89$) and the differences of Gibbs free energies $\Delta\Delta G^{298}$ ($R = -0.85$). Therefore, we replaced E^{HOMO} in the above equation by both parameters (see eqs S2 and S3 of the Supporting Information) and obtained reasonable alternative models without significant statistical deterioration ($R^2 = 0.8954$ with σ^+ and $R^2 = 0.8864$ with $\Delta\Delta G^{298}$; leave-one-out cross-validation, $R^2 = 0.8430$, PRESS = 0.4309 and $R^2 = 0.8530$, PRESS = 0.4502 for σ^+ and $\Delta\Delta G^{298}$, respectively). All data combined indicate that the reaction mechanism of EBDH involves an initial polarization of the substrate, followed by conversion to a carbocation intermediate.

A disadvantage involved in the described multicomponent QSAR analysis is that a complete set of the necessary molecular parameters is only available for 13 of the 20 measured substrates of ethylbenzene dehydrogenase. The only descriptors available for all substrates are those obtained by quantum chemical calculation such as the respective $\Delta\Delta G$ value of carbocation formation. As expected from the previous QSAR analysis, the $\Delta\Delta G$ values alone did not yield a reasonable fit to the measured reaction rates ($R^2 = 0.29$), mainly because the bulkiness of the substrates is not taken into account. However, if the $\Delta\Delta G$ values are combined with just one more descriptor assessing this aspect (molecular refractivity MR, which can be calculated for all 20 substrates in contrast to the Taft constants), QSAR analysis of all 20 measured substrates using only these two descriptors yielded a much improved fit of the data ($R^2 = 0.59$; see Figure S5 of the Supporting Information for correlation plot and equation).

More sophisticated prediction models, which take more variables into consideration and describe changes in reactivity with almost all compounds on the 0.95 R^2 level, have been obtained by artificial neural network analysis of the data and are described elsewhere (*21*).

DISCUSSION

One of the most striking features of ethylbenzene dehydrogenase is its extremely low apparent K_m value for ethylbenzene. This may be rationalized by assuming that ethylbenzene is not present in high abundance in the habitat of strain EbN1, and an enzyme with very high affinity certainly confers it an evolutionary advantage. Moreover, these data suggest that ethylbenzene is indeed the natural substrate of the enzyme. The rather low reaction rate of ethylbenzene oxidation (ca. 150 nmol mg^{-1} min^{-1}) is compensated by the high abundance of the enzyme (up to 10% of total protein in ethylbenzene-grown cells). Moreover, the observed slow reaction rate seems to be characteristic for enzymes involved in anaerobic activation reactions of hydrocarbons or aromatic compounds, since it is in a similar range to those of benzylsuccinate synthase (*22*−*24*) or benzoyl-CoA reductase (*25*).

Remarkably, EBDH exhibits activity with a wide range of alkylaromatic and alkylheterocyclic substrates. Some of them (such as 4-ethylphenol or most of the ethyl-substituted heterocycles) show even higher kinetic rates than recorded for the native substrate. However, in all investigated cases the observed apparent K_m values are much higher than that of ethylbenzene, and the overall catalytic efficiencies (k_{cat}/K_m) clearly indicate that ethylbenzene is the native substrate of the enzyme. The high affinity for ethylbenzene may result from the presence of hydrophobic amino acid residues at the walls of a tunnel leading to the active center, which may facilitate substrate transport into the enzyme interior and discrimination of other compounds (*9*).

The unusual catalytic versatility of EBDH may arise from a rather large active center cavity, which seems not to pose significant steric constraints for para and meta substituents (*9*). Therefore, it was possible to observe activity even with bulky compounds like 4-ethylbiphenyl or 2-ethylnaphthalene.

In all reaction mixtures analyzed by MS, secondary alcohol products were detected. Only in the 1,4-diethylbenzene reaction mixture were two products identified, namely, 1-(4-ethylphenyl)ethanol and 1,1′-(1,4-phenylene)diethanol. The latter compound seems to be produced from 1-(4-ethylphenyl)ethanol as it is present in higher amounts when an excess of ferricenium over substrate is used. This might indicate some preference of the enzyme for 1,4-diethylbenzene over 1-(4-ethylphenyl)ethanol, which is consistent with enzyme inhibition by 1-phenylethanol (see below). The enzyme also seems to require an aromatic system for the specific oxidation of the side chain, although EBDH was previously reported to exhibit activity with substrates such as 3-methyl-2-pentene or ethylidenecyclohexane, which do not contain aromatic rings in their structures (*2*). We repeated the experiments with ethylidenecyclohexane and discovered unspecific reactivity of the enzyme, resulting in trace activity with the ferricenium-based assay and generation of multiple products from hydroxylation and/or water addition reactions. Therefore, ethylidenecyclohexane does not seem to be a real substrate but may mimic a potential transition state of the reaction with aromatic substrates. This may allow the enzyme to bind and convert this compound via different reaction pathways, probably depending on the oxidation state of the molybdenum cofactor. These results also explain the previous observations of enzymic conversion of ethylidenecyclohexane, which were purely based on the detection of products by GC-MS (*2*).

The stereoselectivity of the enzyme with the alternative substrates was not yet investigated and needs further experimental study. Moreover, due to the large dimensions of the active center, the features that make ethylbenzene dehydrogenase so stereoselective in ethylbenzene oxidation cannot be predicted from the structure (*9*). The available structure would principally be consistent with binding of the substrate in either way, allowing both *S* and *R* products to be synthesized.

EBDH is clearly capable of oxidizing not only ethylbenzene but also other aromatic species. It cannot be excluded that strain EbN1 applies the enzyme for activation of other compounds. Therefore, it will be interesting to follow the physiological fate of some of the alcoholic products in strain EbN1. One possibility is that the second enzyme of the ethylbenzene metabolic pathway, phenylethanol dehydrogenase, or another alcohol dehydrogenase may be involved in oxidizing some of these alcohols further to ketones. However, whether strain EbN1 is indeed capable of degrading or transforming ethylbenzene derivatives still needs further examination.

The systematic way of kinetic data analysis enabled by QSAR demonstrated the complexity of factors controlling enzyme reactivity. However, closer inspection of the results shows that a combination of steric, hydrophobic, and electronic features determines the reactivities of alternative substrates. Steric hindrance is described by the Taft constant E_s (respectively molecular refractivity MR). The hydrophobicity/polarity is described by two parameters, hydrophobic constant π and dipole moment μ, which define an optimal range of polarization potential and hydrophobicity of substrates.

Introduction of absolute hardness (η) into the QSAR equation shows that chemically hard substrates generally react slower. This can be due to their higher stability (according to the maximum hardness principle) (*27*) or their lower polarizability. As the proposed mechanism of EBDH (*9*) assumes initial polarization of the ethyl group in the substrate by an aspartate residue (Asp^{223}) of the active site, stronger polarizability (smaller η) may indeed facilitate substrate activation.

However, such an analysis does not distinguish between homolytic and heterolytic cleavage of the C−H bond that would lead to a radical or carbocation intermediate, respectively. The effects of the Hammett constants indicate that the transition state is stabilized by substituents possessing free electron pairs (such as OH or NH_2) in para or ortho position with respect to the ethyl group. This correlation would be consistent with a putative carbocation intermediate but in some cases has also been observed for radical reactions (*26*). Therefore, the $\Delta\Delta G^{298}$ parameters, which supply information on stabilization effects in carbocation formation introduced by modification of the aromatic system, provided valuable information. Equations containing $\Delta\Delta G^{298}$ values yielded the same quality of fit as those containing σ^+ values, which strongly suggests the carbocation nature of the intermediate.

Moreover, the $\Delta\Delta G$ values may even give some explanation about why some ethylbenzene derivatives turned out to be inhibitors. Generally, almost all ΔG^{298} values of carbocation formation of alternative substrates were lower than that of ethylbenzene ($\Delta\Delta G^{298}$ for 4-ethylphenol equal to −46.6 kJ/mol, for 2-ethylthiophene to −26.9 kJ/mol, and for 4-ethylaniline to −96.7 kJ/mol), while those of inhibitors were higher (for example, $\Delta\Delta G^{298}$ values for toluene, 4-ethylpyridine, and 2-methylfuran are 54.8, 68.2, and 28.8 kJ/mol, respectively). The stabilizing effect for a potential carbocation intermediate also depended on the positioning of substituents in the ring, the most beneficial being in para position to the ethyl (or propyl) group.

The inhibition study revealed also an important issue of product inhibition. Judging from its K_i of 20 μM, (*S*)-1-phenylethanol appeared to be a fairly strong competitive inhibitor at first sight. However, one should realize that an inhibitor's strength it is not solely determined by its K_i value but also by its ratio to K_m (which is extremely low in the case of ethylbenzene). From the equation for competitive inhibition by (*S*)-1-phenylethanol given below, it becomes obvious that the low K_m of the substrate decreases significantly the inhibitory influence of (*S*)-1-phenylethanol on overall kinetics.

$$V_i = \frac{V_{max}}{[S] + K_m + \frac{K_m}{K_i}[I]} = \frac{V_{max}}{[S] + K_m + \frac{0.45\,\mu M}{20\,\mu M}[I]} = \frac{V_{max}}{[S] + K_m + 0.0225[I]}$$

Therefore, it is doubtful whether the inhibitory influence of (*S*)-1-phenylethanol has any physiological role, especially since it is transported from the periplasm to the cytoplasm and further converted by phenylethanol dehydrogenase (PED). Apparently, the flux through the metabolic pathway is mainly controlled at the level of the heavily regulated PED, as recently proposed by Höffken et al. (*28*).

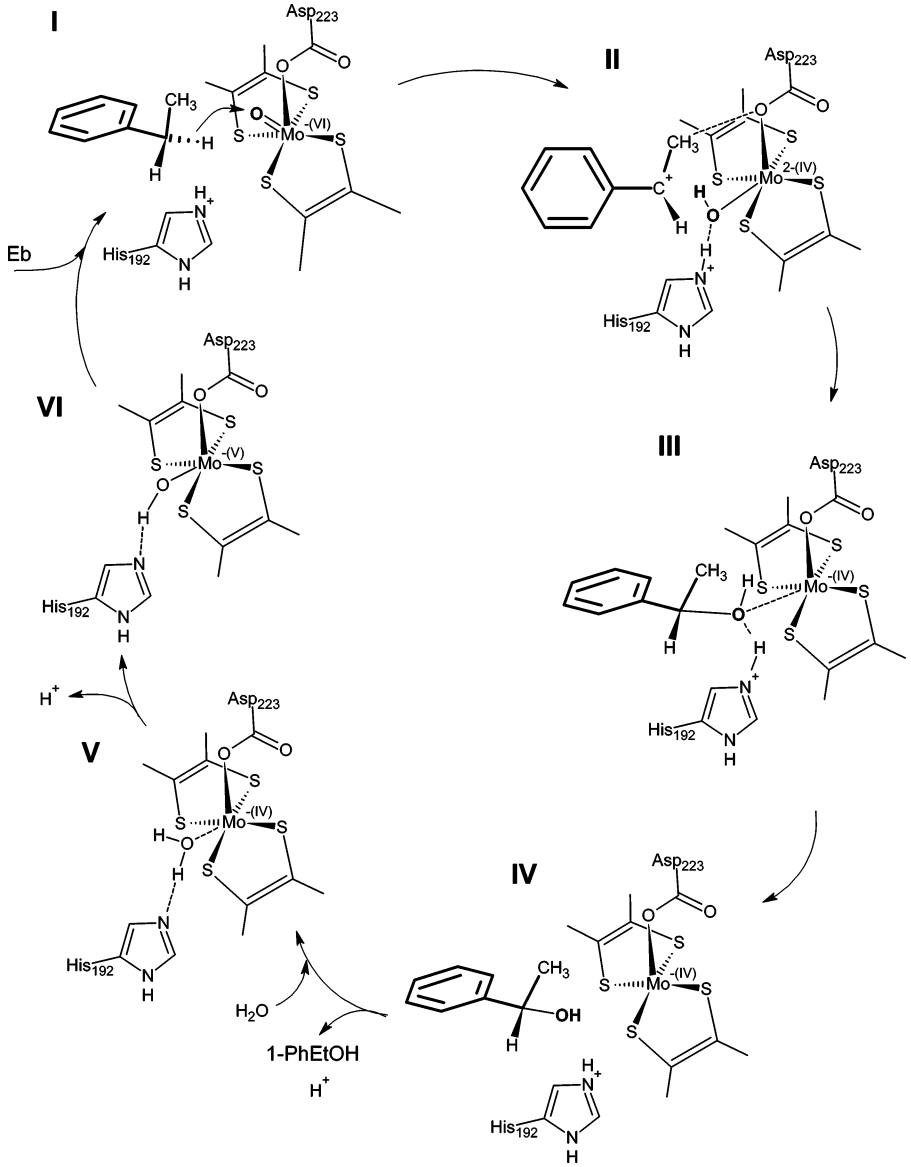

FIGURE 3: Hypothetical mechanism of ethylbenzene oxidation by EBDH. Stage I: Formation of the enzyme−substrate complex with oxidized (Mo^{VI}) molybdenum cofactor. Cleavage of the C−H bond takes place. Stage II: The molybdenum cofactor is reduced (Mo^{IV}), and a carbocation intermediate is formed; His^{192} stabilizes the OH ligand in water-like form. The positive charge of the carbocation is stabilized by interaction with the electron-rich Asp^{223}. Stage III: Nucleophilic attack of the OH group on the carbocation, assisted by His^{192}. Stage IV: Product formation and release; deprotonation of His^{192}. Stage V: Coordination of a water molecule to reduced molybdenum cofactor and formation of a hydrogen bond with His^{192}. Stage VI: Abstraction of protons from the water ligand with parallel oxidation of the molybdenum active site.

On the basis of the analysis of kinetic data and the recently published EBDH structure, one can propose a hypothetic reaction mechanism of EBDH. It is apparent that EBDH requires an aromatic system that stabilizes the positive charge in order to activate the alkyl chain of the substrate. The active site is a relatively wide channel of approximately 7 Å diameter in the α-subunit of EBDH. It is filled with a range of aromatic (Trp^{87}, Trp^{481}, Tyr^{483}, His^{192}, Phe^{446}) and hydrophobic (Ile^{85}, Ile^{221}) amino acids that provide convenient polarity for hydrophobic, aromatic substrates. At the moment it is not clear which of these amino acid residues are involved in the catalytic process. However, Asp^{223} (also coordinating the molybdenum) and His^{192} seem to be in the best position to take part in the hydrocarbon activation process, together with the molybdenum oxo ligand that is expected to be present in the oxidized form of EBDH. Most probably, the Mo═O ligand together with His^{192} is responsible for carbocation formation. Activation may proceed via subtraction of a proton from C2 of ethylbenzene with simultaneous transfer of the electron pair (Figure 3, stage I). The positive charge of the carbocation may be stabilized by the aromatic system but also by the Asp^{223} (or less likely Asn^{218}) residue (Figure 3, stage II). Our theoretical calculations (data not shown) suggest that, in the Mo(IV) state, a H_2O group is stable as a molybdenum ligand. Therefore, most probably, the subtracted proton is localized on the oxo ligand, and a hydrogen bond with protonated His^{192} is formed. Consequently, the OH ligand acts as the nucleophile and attacks the carbocation, which may be further facilitated by the His residue (Figure 3, stage III). Our preliminary calculations suggest strong repulsion between His−Nϵ and the Mo═O ligand when the nitrogen atom is deprotonated, forcing the His residue to stay out of the catalytic site. Therefore, His−Nϵ of the imidazole ring should be proto-

nated in the beginning of the catalytic cycle, forming a His−NH···O═Mo hydrogen bond.

Finally, the product and a proton are released, and a water molecule coordinates to the reduced molybdenum cofactor (Figure 2, stage V). The electrons will be transferred from the molybdenum cofactor via the iron−sulfur clusters to the heme *b* cofactor of the γ-subunit and the active site reoxidized. During the change of oxidation state of the molybdenum from stage IV to stage V and then to stage VI, protons must be removed from the water ligand (possibly through transfer to His^{192} and then to bulk solvent), resulting in restoring the catalytically active Mo═O ligand (Figure 3, stages V and VI) and the protonated His^{192} residue.

The mechanism presented above explains the high stereospecificity of EBDH in oxidation of ethylbenzene. The reaction would be predicted to retain the stereochemistry, i.e., the *pro-S* hydrogen of C2 of ethylbenzene would be removed and replaced by the OH group to yield (*S*)-1-phenylethanol. Even if rotation between the ring and ethyl group is theoretically possible in such a big active center, the coordination of substrate with the ethyl group pointing downward and hydrogen atoms pointing upward would certainly make the reaction harder to proceed. The proposed mechanism provides a scaffold for experiments to test this hypothesis. The detailed quantum chemical computational verification of the proposed mechanism against possible radical alternatives [with a substrate-derived radical intermediate and Mo(V)−OH cofactor] is also planned.

Finally, it is significant that we achieved promising conversion of ethylbenzene in the electrochemical reactor. The system provides a basis for further studies that will focus on application of EBDH in fine chemical synthesis. Recycling of ferricenium makes the whole synthesis much cheaper and faster due to the constant high concentration of the reoxidation agent.

SUPPORTING INFORMATION AVAILABLE

Michaelis−Menten curve fits of EBDH activity with ethylbenzene (Figure S1) and ferricenium (Figure S2) as substrates, structures of compounds tested as EBDH substrates (Figure S3), Lineweaver−Burk plot for (S)-1-phenylethanol (Figure S4), correlation plot for QSAR model with MR and $\Delta\Delta G$ (Figure S5), and additional QSAR equations (eqs S1−S3). This material is available free of charge via the Internet at http://pubs.acs.org.

REFERENCES

1. Hille, R. (1996) The mononuclear molybdenum enzymes, *Chem. Rev. 96*, 2757−2816.
2. Johnson, H. A., Pelletier, D. A., and Spormann, A. M. (2001) Isolation and characterization of anaerobic ethylbenzene dehydrogenase, a novel Mo-Fe-S enzyme, *J. Bacteriol. 183*, 4536−4542.
3. Kniemeyer, O., and Heider, J. (2001) Ethylbenzene dehydrogenase, a novel hydrocarbon-oxidizing molybdenum/iron-sulfur/heme enzyme, *J. Biol. Chem. 276*, 21381−21386.
4. Rabus, R., Kube, M., Beck, A., Widdel, F., and Reinhardt, R. (2002) Genes involved in the anaerobic degradation of ethylbenzene in a denitrifying bacterium, strain EbN1, *Arch. Microbiol. 178*, 506−516.
5. Krafft, T., Bowen, A., Theis, F., and Macy, J. M. (2000) Cloning and sequencing of the genes encoding the periplasmic-cytochrome B-containing selenate reductase of *Thauera selenatis*, *DNA Sequence 10*, 365−377.
6. McDevitt, C. A., Hugenholtz, P., Hanson, G. R., and McEwan, A. G. (2002) Molecular analysis of dimethyl sulphide dehydrogenase from *Rhodovulum sulfidophilum*: its place in the dimethyl sulphoxide reductase family of microbial molybdopterin-containing enzymes, *Mol. Microbiol. 44*, 1575−1587.
7. Lledo, B., Martinez-Espinosa, R. M., Marhuenda-Egea, F. C., and Bonete, M. J. (2004) Respiratory nitrate reductase from haloarchaeon *Haloferax mediterranei*: biochemical and genetic analysis, *Biochim. Biophys. Acta 1674*, 50−59.
8. Yoshimatsu, K., Iwasaki, T., and Fujiwara, T. (2002) Sequence and electron paramagnetic resonance analyses of nitrate reductase NarGH from a denitrifying halophilic euryarchaeote *Haloarcula marismortui*, *FEBS Lett. 516*, 145−150.
9. Kloer, D. P., Hagel, C., Heider, J., and Schulz, G. E. (2006) Crystal structure of ethylbenzene dehydrogenase from *Aromatoleum aromaticum*, *Structure 14*, *1377−1388*.
10. Szaleniec, M., Jobst, B., and Heider, J. (2003) Ethylbenzene dehydrogenase: oxidation of hydrocarbons without oxygen, *Ann. Pol. Chem. Soc.*, 240−245.
11. Frisch, M. J., Trucks, G. W., Schlegel, H. B., Scuseria, G. E., Robb, M. A., Cheeseman, J. R., Montgomery, J. A., Jr., Vreven, T., Kudin, K. N., Burant, J. C., Millam, J. M., Iyengar, S. S., Tomasi, J., Barone, V., Mennucci, B., Cossi, M., Scalmani, G., Rega, N., Petersson, G. A., Nakatsuji, H., Hada, M., Ehara, M., Toyota, K., Fukuda, R., Hasegawa, J., Ishida, M., Nakajima, T., Honda, Y., Kitao, O., Nakai, H., Klene, M., Li, X., Knox, J. E., Hratchian, H. P., Cross, J. B., Adamo, C., Jaramillo, J., Gomperts, R., Stratmann, R. E., Yazyev, O., Austin, A. J., Cammi, R., Pomelli, C., Ochterski, J. W., Ayala, P. Y., Morokuma, K., Voth, G. A., Salvador, P., Dannenberg, J. J., Zakrzewski, V. G., Dapprich, S., Daniels, A. D., Strain, M. C., Farkas, O., Malick, D. K., Rabuck, A. D., Raghavachari, K., Foresman, J. B., Ortiz, J. V., Cui, Q., Baboul, A. G., Clifford, S., Cioslowski, J., Stefanov, B. B., Liu, G., Liashenko, A., Piskorz, P., Komaromi, I., Martin, R. L., Fox, D. J., Keith, T., Al-Laham, M. A., Peng, C. Y., Nanayakkara, A., Challacombe, M., Gill, P. M. W., Johnson, B., Chen, W., Wong, M. W., Gonzalez, C., and Pople, J. A. (2003) Gaussian 03, revision C.02, Gaussian, Inc., Pittsburgh, PA.
12. Hansch, C., and Alber, L. (1995) *Exploring QSAR Fundamentals and Application in Chemistry and Biology*, ACS Processional Reference Book, American Chemical Society, Washington, DC.
13. Fujita, T., Iwasa, J., and Hansch, C. (1964) A new substituent constant, π, derived from partition coefficients, *J. Am. Chem. Soc. 86*, 5175−5180.
14. Okamoto, Y., and Brown, H. C. (1957) A quantitative treatment for electrophilic reactions of aromatic derivatives, *J. Org. Chem. 22*, 485−494.
15. Accelrys, Inc. (2005) Cerius2 Modeling Environment, Release 4.8, Accelrys Software Inc., San Diego.
16. Stein, S. E. (2005) Mass Spectra, in *NIST Chemistry WebBook* (Linstrom, P. J., and Mallard, W. G., Eds.) NIST Standard Reference Database Number 69, National Institute of Standards and Technology, Gaithersburg, MD, 20899 (http://webbook. nist. gov).
17. Johnstone, R. A. W., and Rose, M. E. (1996) Structure elucidation, in *Mass Spectrometry for Chemist and Biochemists*, 2nd ed., pp 325−395, Press Syndicate of the University of Cambridge, Cambridge.
18. Cornish-Bowden, A. (1995) *Analysis of Enzyme Kinetic Data*, Oxford University Press, New York.
19. Singh, P. P., Srivastava, H. K., and Pash, F. A. (2004) DFT-based QSAR study of testosterone and its derivatives, *Bioorg. Med. Chem. 12*, 171−177.
20. Arnett, E. M., and Ludwig, R. T. (1995) On the relevance of the Parr-Pearson principle of absolute hardness to organic chemistry, *J. Am. Chem. Soc. 117*, 6627−6628.
21. Szaleniec, M., Witko, M., Tadeusiewicz, R., and Goclon, J. (2006) Application of artificial neural networks and DFT-based parameters for prediction of reaction kinetics of ethylbenzene dehydrogenase, *J. Comput.-Aided Mol. Des. 20*, 145−157.
22. Biegert, T., Fuchs, G., and Heider, J. (1996) Evidence that oxidation of toluene in the denitrifying bacterium *Thauera aromatica* is initiated by formation of benzylsuccinate from toluene and fumarate, *Eur. J. Biochem. 238*, 661−668.
23. Verfürth, K., Pierik, A. J., Leutwein, C., Zorn, S., and Heider, J. (2004) Substrate specificities and electron paramagnetic resonance properties of benzylsuccinate synthases in anaerobic toluene and *m*-xylene metabolism, *Arch. Microbiol. 181*, 155−162.

24. Krieger, C. J., Beller, H. R., Reinhard, M., and Spormann, A. M. (1999) Initial reactions in anaerobic oxidation of m-xylene by the denitrifying bacterium *Azoarcus* sp. strain T, *J. Bacteriol. 181*, 6403−6410.
25. Boll, M., and Fuchs, G. (1995) Benzoyl-coenzyme A reductase (dearomatizing), a key enzyme of anaerobic aromatic metabolism, *Eur. J. Biochem. 234*, 921−933.
26. Hansch, C., and Gao, H. (1997) Comparative QSAR: Radical reactions of benzene derivatives in chemistry and biology, *Chem. Rev. 97*, 2995−3059.
27. Pearson, R. G. (1987) Recent advances in the concept of hard and soft acids and bases, *J. Chem. Educ. 64*, 561−567.
28. Höffken, H. W., Duong, M., Friedrich, T., Breuer, M., Hauer, B., Reinhardt, R., Rabus, R., and Heider, J. (2006) Crystal structure and enzyme kinetics of the (*S*)-specific 1-phenylethanol dehydrogenase of the denitrifying bacterium strain EbN1, *Biochemistry 45*, 82−93.

BI700633C